Water Science and Engineering 2023, 16(2): 154−164

HOSTED BY

ELSEVIER

Available online at www.sciencedirect.com

Water Science and Engineering

journal homepage: wse.hhu.edu.cn

Understanding association between methylene blue dye and biosorbent: Palmyrah sprout casing in adsorption process in aqueous phase

D.M.N.H. Jayasuriya, Kannan Nadarajah*

Department of Agricultural Engineering, Faculty of Agriculture, University of Jaffna, Ariviyal Nagar, Kilinochchi 44000, Sri Lanka

Received 27 July 2022; accepted 20 December 2022
Available online 5 January 2023

Abstract

Water pollution caused by industrial dyes has become a severe problem in the modern world. Biosorbents can be used in an eco-friendly manner to remove industrial dyes. In this study, five biosorbents were selected: palmyrah sprout casing (PSC), manioc peel, lime peel, king coconut husk, and coconut kernel. Batch adsorption experiments were conducted to identify the best biosorbent with the highest ability to adsorb methylene blue (MB) from wastewater. The detailed mechanisms of PSC used in the adsorptive removal of MB in aqueous phase were investigated. Of the five biosorbents, PSC exhibited the best removal performance with an adsorption capacity at equilibrium (q_e) of 27.67 mg/g. The q_e values of lime peel, king coconut husk, manioc peel, and coconut kernel were 24.25 mg/g, 15.29 mg/g, 10.84 mg/g, and 7.06 mg/g, respectively. To explain the mechanisms of MB adsorption with the selected biosorbents, the Fourier transform infrared (FTIR) spectrometry and X-ray diffraction (XRD) analyses were performed to characterize functional properties, and isotherm, kinetic, rate-limiting, and thermodynamic analyses were conducted. The FTIR analysis revealed that different biosorbents had different functional properties on their adsorptive surfaces. The FTIR and XRD results obtained before and after MB adsorption with PSC indicated that the surface functional groups of carbonyl and hydroxyl actively participated in the removal process. According to the isotherm analysis, monolayer adsorption was observed with the Langmuir model with a determination coefficient of 0.998. The duration to reach the maximum adsorption capacity for MB adsorption with PSC was 120 min, and the adsorption process was exothermic due to the negative enthalpy change (−9.950 kJ/mol). Moreover, the boundary layer thickness and intraparticle diffusion were the rate-limiting factors in the adsorption process. As a new biosorbent for MB adsorption, PSC could be used in activated carbon production to enhance the performance of dye removal.

Keywords: Biosorbents; Isotherm; Kinetics; Methylene blue; Rate-limiting factor; Thermodynamics

1. Introduction

Industrial dyes significantly pollute freshwater sources. Different types of dyes are used in large quantities for various industrial applications, such as cosmetics, textiles, food industry, and paper printing. Around 100 000 dyes are commercially available, and more than 7 107 t of dyes are annually generated worldwide (Benkhaya et al., 2018). These dyes are extremely toxic and negatively influence natural environmental processes. Approximately 11 000 harmful dyes are discarded into freshwater sources, causing deterioration of water quality (Rehman et al., 2019). Various chemical and physical techniques have been used for wastewater treatments, such as electrochemical treatment, biodegradation, photochemical degradation, bacterial decolorization, coagulation, flocculation, and membrane separation (Rani et al., 2017). However, compared to other methods, adsorption is a reasonable strategy due to its versatility, high efficiency, and ease of use. Moreover, activated carbon has been widely used for the adsorptive removal of various dyes, but the commercially available activated carbon is highly expensive, and it has problems with regeneration. Therefore, many industries look

* Corresponding author.
E-mail address: nkannan@univ.jfn.ac.lk (Kannan Nadarajah).
Peer review under responsibility of Hohai University.

https://doi.org/10.1016/j.wse.2022.12.006

for cost-effective adsorbents to efficiently remove various dyes (Stjepanovic et al., 2021). Considering the efficiency and cost, biomass-based adsorbents (biosorbents) are a reasonable alternative to activated carbon (Park et al., 2010). They are widely available and relatively cheap and require little or no processing (Stjepanović et al., 2021).

Methylene blue (MB) is an organic cationic dye that has been widely used in many industrial operations, such as wool, cotton, silk, and acrylic production. Even though it is not much hazardous, it generates some harmful impacts to human, such as vomiting, cyanosis, shock, increase of heart rate, necrosis of tissues, and jaundice (Bhatti et al., 2012). Therefore, it must be removed from the industrial effluent with cost-effective strategies. A number of biosorbents have been tested to achieve this target, such as banana peel (Amela et al., 2012), banana stem powder (Ahmad et al., 2016), the peel of yellow passion fruit, mandarin peel (Pavan et al., 2007), garlic straw (Kallel et al., 2016), the peel of citrus fruit (Dutta et al., 2011), and watermelon rind (Lakshmipathy and Sarada, 2015). Moreover, the removal of crystal violet dye with eucalyptus leaves has been successfully studied. The removal capacity of the acid modification of eucalyptus leaves with phosphoric acid improved the adsorptive capacity to 141 mg/g (Ghosh et al., 2021c). In addition, coconut coir has been used to remove Safranin-O dye with some modifications using acids (phosphoric acid and sulfuric acid), which showed greater than 98% removal of Safranin-O dye at concentrations less than 200 mg/L (Ghosh et al., 2021a). It has also been reported that eucalyptus leaves were successfully used with phosphoric acid modification for the removal of MB dye from water, and the acid-treated eucalyptus leaves achieved a removal capacity of 194.34 mg/g (Ghosh et al., 2019). Furthermore, phosphoric acid modification of bamboo leaves achieved an adsorption performance of 168.339 mg/g at 318 K for toxic malachite green (Ghosh et al., 2022).

Additionally, a comparative batch adsorption experiment was performed to remove toxic MB dye with untreated *Lathyrus sativus* husk, the husk treated with 0.500 mol/L of H_2SO_4, and the husk treated with 0.333 mol/L of H_3PO_4, which achieved adsorption performances of 98.33 mg/g, 104.28 mg/g, and 113.25 mg/g at 303 K, respectively. Due to the development of surface functional groups, the phosphoric acid treatment yielded the highest adsorption performance (113.25 mg/g) (Ghosh et al., 2021b). These results clearly showed that the adsorption performances of different biosorbents can be improved by some chemical treatments that are responsible for the modification of functional groups. Therefore, appropriate modification methods are required to improve the adsorption performance of the biosorbents used to remove dyes from water.

The adsorption process has two materials: adsorbent and adsorbate. Adsorbents are the materials with the ability to attract other possible substances, which are called adsorbates (Zhao et al., 2021). The rate of removal of adsorbates with adsorbents is controlled by many factors, such as the surface functional properties of adsorbents and the nature of the media in which the adsorption process takes place. The adsorbent dosage, pH, temperature, and initial concentration are major considerations as far as the adsorption environment is concerned (Zhao et al., 2021). The surface functional properties, such as the nature and distribution of functional groups and the hydrophilic or hydrophobic nature of adsorbent sites, are also critical to the removal of different pollutants. The pollutants with negatively-charged surfaces can be effectively removed by the absorbents with positively-charged surfaces, and vice versa (Nadarajah et al., 2021). Therefore, it is important to evaluate the adsorption system and the interaction between adsorbates and adsorbents to achieve reasonable adsorptive removal performance of the adsorbents concerned for a particular case.

There are many locally available biosorbents that have not yet been scientifically tested for their adsorption abilities of MB dye from industrial wastewater. Therefore, this study investigated the adsorption performances of five novel biosorbents: palmyrah sprout casing (PSC), manioc peel, lime peel, king coconut husk, and coconut kernel. Afterwards, the impacts of adsorbent dosage, MB concentration, temperature, and solution pH on the adsorptive removal process were analyzed. Moreover, isotherm, kinetics, thermodynamics, and rate-limiting factors were analyzed to properly interpret the mechanisms of MB adsorption with the biosorbents.

2. Materials and methodology

2.1. Materials

The chemicals, such as MB, hydrochloric acid (HCl), sodium hydroxide (NaOH), and sodium chloride (NaCl), were obtained with high-purity percentages, and they were used as purchased without further purification. MB was purchased from the Winlab Ltd. Company. Five locally available biosorbents were selected: the sprout casing of palmyrah (*Borassus flabellifer*), the husk of king coconut (*Cocos nucifera* var. *aurantiaca*), the peel of cassava (*Manihot esculenta*), the peel of lime (*Citrus aurantiifolia*), and the remaining kernel after milk extraction from coconut flesh (*Cocos nucifera*). They have not been previously tested for their adsorption abilities of MB. These materials were collected from a vegetable market in Kilinochchi, Northern Province, Sri Lanka and supplied by local farmers. The collection process was carefully performed to maintain the purity of the samples.

2.2. Preparation of biosorbents

Collected biosorbents were cut into smaller pieces and washed with distilled water to remove impurities and water-soluble compounds. Washed materials were dried using an oven at 105°C until a constant weight was obtained (Amela et al., 2012). Dried materials were ground and sieved with sieves in mesh sizes of 2 mm and 1 mm to obtain particle sizes between 1 mm and 2 mm (Low and Tan, 2018). Sieved particles were stored in glass bottles and used for experiments. Fig. 1 shows the prepared biosorbents.

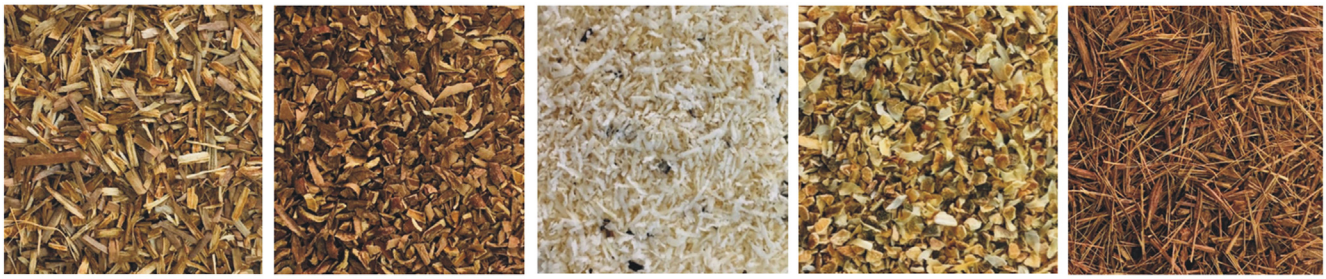

(a) PSC (b) Manioc peel (c) Coconut kernel (d) Lime peel (e) King coconut husk

Fig. 1. Biosorbent particles used in experiments.

2.3. Adsorption experiments

Adsorption experiments were conducted to identify the best biosorbent among the selected biosorbents with the highest adsorption ability to remove MB dye. Appendix A shows the detailed experimental procedures.

2.4. Characterization of biosorbents

2.4.1. Surface charge analysis

Experiments were conducted to estimate the point of zero charge (pH_{pzc}) in order to find the pH value at which surface charges of the selected biosorbents are equal to zero. The pH_{pzc} values of the biosorbents were estimated using the pH drift method (Vijayakumar et al., 2009). NaCl solution was prepared with a concentration of 0.01 mol/L, and its pH was altered between 3 and 9 by adding either NaOH or HCl. After initial pH was stabilized, accurately weighed 0.2 g of each biosorbent was added to 20 mL of the solution. Two replicates were used. The samples were kept in a shaking incubator operated at 30°C and 150 r/min. After 24 h, final pH was recorded. A graph was then developed by considering initial and final pH values, and pH_{pzc} was obtained for each biosorbent. Fig. A.1 in Appendix A shows the pH_{pzc} graph.

2.4.2. Analyses of surface functional groups and crystallographic features

An alpha Fourier transform infrared (FTIR) spectrometer (BRUKER, ALPHA II) was used to analyze surface functional groups. FTIR readings were collected within a spectral range of 4 000−600 cm^{-1} at a resolution of 4 cm^{-1} with 32 average scans. The crystallographic features of the selected biosorbents were analyzed with an X-ray diffractometer (XRD; PANalytical, AERIS). Manioc peel, coconut kernel, lime peel, PSC, and king coconut husk were analyzed to identify the differences among them. PSC was especially analyzed before and after MB adsorption to examine the changes in surface functional groups and crystallographic features resulting from adsorption.

2.5. Effects of experimental conditions

The effects of the experimental conditions, such as pH, biosorbent dosage, initial dye concentration, and temperature, were investigated with several experiments. The tested pH ranged from 3 to 11. The influence of the initial MB concentration was tested within a range from 50 mg/L to 500 mg/L. The selected range of the biosorbent dosage was from 1 g/L to 20 g/L. The influence of temperature was investigated between 30°C and 50°C. When an experiment was conducted for a particular experimental condition, other experimental conditions were maintained at the same values (a biosorbent dosage of 3 g/L, an initial dye concentration of 100 mg/L, a pH value of 6, and a temperature of 303 K), and only the examined factor was changed within the selected range. Required conditions were achieved with a shaking incubator operated at 150 r/min. Each experiment was performed for 24 h to achieve equilibrium conditions. After 24 h, centrifugation was conducted for 5 min at 10 000 r/min to separate the supernatant.

2.6. Isotherm, kinetic, rate-limiting factor, and thermodynamic analyses

The Freundlich, Langmuir, and Temkin models were used for isotherm analysis. For adsorption kinetic analysis, the pseudo-first-order, pseudo-second-order, and Elovich kinetic models were used. The MB concentrations of 100 mg/L, 300 mg/L, and 500 mg/L were used for kinetic investigation. The Van't Hoff equation was used for thermodynamic analysis. The experimental data for investigation of the effect of different temperatures on adsorption was used for thermodynamic analysis. Kinetic experimental data were used to analyze the rate-limiting factors with the Weber−Morris model. The relevant equations of the aforementioned models are shown in Appendix A.

3. Results and discussion

3.1. Adsorptive experiments

Comparison of the selected biosorbents was conducted according to their MB adsorption performances. As shown in Fig. 2, PSC exhibited the highest MB adsorption performance. Therefore, PSC was selected as the best biosorbent among the five biosorbents for MB removal, and it was used for further adsorption experiments. PSC obtained an adsorption capacity at equilibrium (q_e) of (27.67 ± 0.05) mg/g and a removal efficiency of 83.02% ± 0.15%. The lowest q_e ((7.05 ± 0.25) mg/g) and

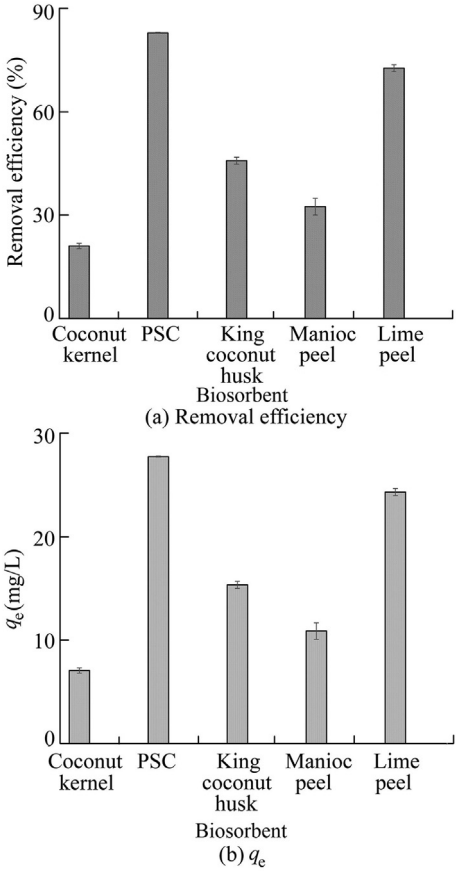

Fig. 2. Removal efficiency and q_e values of selected biosorbents for MB adsorption.

removal efficiency (21.16% ± 0.76%) were reported for coconut kernel. The q_e values of lime peel, king coconut husk, and manioc peel were (24.25 ± 0.33) mg/g, (15.29 ± 0.33) mg/g, and (10.84 ± 0.80) mg/g, respectively. The removal efficiencies of lime peel, king coconut, and manioc peel were 72.77% ± 1.01%, 45.89% ± 1.01%, and 32.54% ± 2.40%, respectively. The variations in the adsorption performances of the selected biosorbents were due to the differences in the identified characteristics. As revealed by the XRD and FTIR analyses in Sections 3.2.2 and 3.2.3, their surface functional properties were different from each other. According to the results obtained from the point of zero charge experiment (Section 3.2.1), their net surface charges were also different. Adsorption is a process that is mainly influenced by the surface characteristics of adsorbents. Therefore, such differences could be the key reasons for the variations in the adsorption performances of the selected five biosorbents.

3.2. Characterization of biosorbents

3.2.1. Point of zero charge

pH_{pzc} is related to the surface charge analysis of adsorbents. It is developed based on the isoelectric point of the surface of the adsorbent (Kallel et al., 2016). According to the concept of pH_{pzc}, the net surface charge of adsorbents can be positive, negative, or neutral according to the pH of the adsorption system. At the point where the pH of the solution is equal to pH_{pzc}, the net charge on the surface of the adsorbent is zero (neutral). The surface charge of the adsorbent becomes positive at a pH value less than pH_{pzc}. When the pH of the medium is higher than pH_{pzc}, the net charge of the adsorbent surface becomes negative (Shakoor and Nasar, 2016). Fig. A.1 in Appendix A shows ΔpH (initial pH minus final pH) versus initial pH, where pH_{pzc} is taken as the point that intercepts the horizontal axis (Dahri et al., 2015). The pH_{pzc} values of PSC, coconut kernel, king coconut husk, manioc peel, and lime peel were 6.15, 5.38, 4.64, 6.47, and 5.38, respectively.

The pH_{pzc} values of the selected biosorbents showed their differences in surface charge distributions. This also explained their different adsorption capacities during the adsorption experiments for the selection of the best biosorbent. Changes in surface charge with varying pH values play an important role in the electrostatic interactions involved in the adsorption process. Positively charged ions or molecules are attracted to negatively charged surfaces, while ions or molecules with negative charges are attracted to positively charged surfaces due to the electrostatic interactions (Dahri et al., 2015). MB is classified under cationic dyes. Therefore, an effective performance of adsorptive removal of MB could be expected at pH values higher than pH_{pzc} of the adsorbent. At pH values less than pH_{pzc}, the surface of the adsorbent could be protonated. As a result, repulsive forces could be active between the positively charged adsorbent surface (H^+) and dye cations (Kallel et al., 2016). Thus, poor removal capacities could be achieved at pH values lower than pH_{pzc}.

3.2.2. Surface functional groups

MB adsorption onto the selected biosorbent was influenced by the interactions among functional groups present on the surfaces of the adsorbent and MB dye. As shown in Fig. 3(a), a small peak was identified at 726.96 cm^{-1} on the spectrum of coconut kernel, representing C═C bending related to alkene. Other tested biosorbents did not significantly show this peak. Another peak was observed on the spectra of PSC, manioc peel, lime peel, and king coconut husk at 1 048.22 cm^{-1}, indicating CO−O−CO stretching in anhydride. Coconut kernel did not significantly show this peak. A large peak was observed for coconut kernel within a range from 1 720 cm^{-1} to 1 740 cm^{-1}, indicating the associaion with C═O stretching related to aldehydes. Comparatively smaller peaks were observed for king coconut husk and lime peel in the same region. For PSC and manioc peel, even much smaller peaks than other biosorbents were observed within that region. A peak related to carbon dioxide (2 349 cm^{-1}) was observed for king coconut husk and PSC, and it was light for lime peel. Coconut kernel and manioc peel did not show significant peaks at that wave length. Two considerable peaks were identified on the coconut kernel spectrum in the range from 2 840 cm^{-1} to 3 000 cm^{-1}. This region was related to C−H stretching in alkane, and this significant peak was not identified for other biosorbents within this region. Functional groups that contain oxygen, such as alcoholic −OH streching and carbonyl groups, were found within a range of 1 240−1 670 cm^{-1}

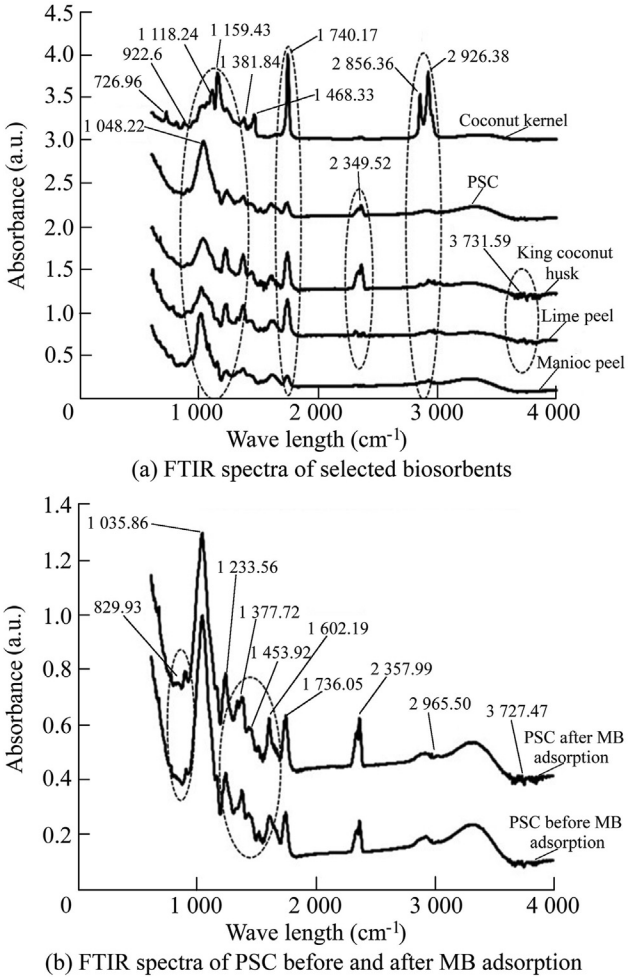

(a) FTIR spectra of selected biosorbents

(b) FTIR spectra of PSC before and after MB adsorption

Fig. 3. FTIR spectra of selected biosorbents and FTIR spectra of PSC before and after MB adsorption.

(Nadarajah et al., 2021). The changes in the spectra of the studied biosorbents in this region indicated the differences in their oxygen containing functional groups. Adsorption is a surface-related process that is influenced by various functional groups on the surfaces of biosorbents. Therefore, the identified differences in the functional groups of these five selected biosorbents were responsible for their different MB adsorption capacities.

FTIR investigation was also performed for PSC to study the contribution of surface functional groups to adsorption removal of MB from the dye solution. As shown in Fig. 3(b), some changes occurred on the functional groups of PSC due to MB adsorption. A slight peak occurred at 829.93 cm^{-1} after MB adsorption, indicating the change in C−H bending due to MB adsorption. The comparison of the scenarios before and after MB adsorption showed that visible changes appeared within a region from 1 300 cm^{-1} to 1 600 cm^{-1}, which included N−O stretching in nitro compounds and C−H bending in aldehyde and alkanes. The observed changes after the adsorption within a range from 1 240 cm^{-1} to 1 670 cm^{-1} were due to the changes in the functional groups containing oxygen. Thus, the functional groups containing oxygen (hydroxyl, carbonyl, C−H bending, and N−O stretching) actively participated in the adsorption mechanisms. Hence, the aforementioned functional groups should be enriched to enhance the adsorption capacity of PSC with some modification techniques.

3.2.3. Carbon structure

XRD analysis reveals the information relevant to the chemical composition of biomass and how it interacts with dye molecules. Fig. 4(a) shows the XRD spectra of the selected biosorbents. The visible differences in the XRD spectra of the biosorbents indicated that their crystallographic features were not similar. A slight peak observed at $2\theta = 15.1°$ (with θ denoting the diffraction angle) on the spectrum of manioc peel and at $2\theta = 22.4°$ on king coconut husk, representing the cellulose structure (Nadarajah et al., 2021). No significant peak was identified on the spectra of PSC, coconut kernel, and lime peel due to their cellulose structures. These differences could be related to the variations in the microcrystalline structures of cellulose in the selected biosorbents and cellulosic compounds with active −OH (Nadarajah et al., 2021). Such differences in the crystalline features of these biosorbents explained their different adsorption capacities during the adsorption experiments.

To study the involvement of crystallographic features in the MB adsorption process with PSC, XRD analysis was perfomed before and after the adsorption. As shown in Fig. 4(b), the crystal structure of PSC exhibited significant differences after MB adsorption. These changes were due to the binding of MB onto the adsorbent or the formation of new compounds resulting from MB adsorption (Khan et al., 2019).

3.3. Effects of experimental conditions

3.3.1. Influence of initial pH

Fig. 5 shows the change in q_e within a pH range from 3 to 11. As pH was increased from 3.19 to 4.00, q_e increased from (19.50 ± 0.30) mg/g to (25.90 ± 0.43) mg/g. However, q_e did not change significantly after pH exceeded 4.08. Dye adsorption was almost retained at a constant level at high pH values. A similar pattern was reported for MB adsorption with garlic peel (Hameed and Ahmad, 2009), *Casuarina equisetifolia* needle (Dahri et al., 2015), and the peel of *Citrus limetta* fruit (Shakoor and Nasar, 2016).

The change in solution pH affects the surface charges of adsorbents through the protonation and deprotonation processes (Kallel et al., 2016). The surface of adsorbents could be attacked by H^+ ions at low pH values, causing some repulsive forces with the cationic dye MB. Therefore, the interactions between the adsorption sites of PSC and MB ions decreased at low pH values due to the high mobility and concentration of H^+ ions. On the other hand, H^+ concentration could be low at high pH values. Therefore, the competition for dye cations is low (Amela et al., 2012).

The pH_{pzc} concept can also explain the influence of pH on the adsorption behavior. The pH_{pzc} value of PSC was 6.15. Therefore, the net surface charges on the adsorbent became

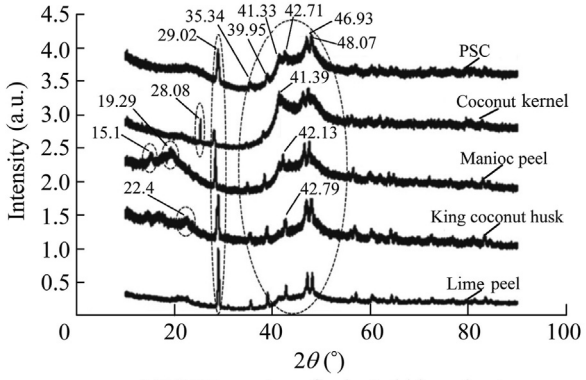

(a) XRD spectra of selected biosorbents

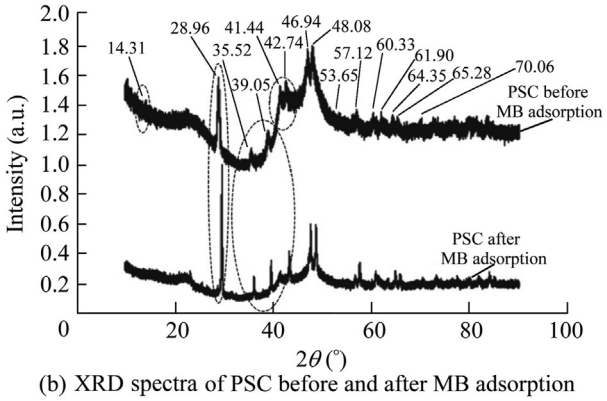

(b) XRD spectra of PSC before and after MB adsorption

Fig. 4. XRD spectra of selected biosorbents and XRD spectra of PSC before and after MB adsorption.

negative at pH values higher than 6.15 (Vijayakumar et al., 2009). Thus, pH values above pH_{pzc} are favorable for cationic dye adsorption due to the electrostatic attractions developed between the adsorbate and adsorbent (Dahri et al., 2015).

3.3.2. Effect of initial MB concentration

The initial dye concentration played a major role in the dye adsorption performance. To overcome the resistance for mass transfer of molecules from aqueous phase to solid phase, necessary driving forces are provided by the initial concentration of the adsorbate (Hameed and Ahmad, 2009). Fig. 6 shows the influence of initial MB concentration on the dye removal process. As the initial dye concentration was increased, the amount of dye removed at equilibrium (q_e) increased, but the removal efficiency decreased. These findings agreed with previous studies on MB removal with the skin of bamboo shoot (Zhu et al., 2019) and rice husk (Labaran et al., 2019).

The increase in q_e with the initial MB concentration was due to the high contact probability between the adsorbent and adsorbate at high initial concentrations (Nadarajah et al., 2021). As the initial MB concentration was increased from 50 mg/L to 200 mg/L, q_e significantly increased from (15.81 ± 0.20) mg/g to (48.27 ± 0.17) mg/g. After the initial MB concentration exceeded 200 mg/L, further increment in the MB concentration did not cause a significant increase in q_e, and q_e gradually reached equilibrium. The highest adsorption capacity (54.13 mg/g) was obtained with an initial MB concentration of 500 mg/L. This variation pattern of q_e was due to the presence of many unoccupied active sites on the adsorbent surface at low dye concentrations. When the dye concentration was increased, the availability of free active sites decreased (Etim et al., 2016). However, the removal efficiency showed an opposite behavior to q_e. As the initial MB concentration was increased from 50 mg/L to 500 mg/L, the removal efficiency gradually decreased from 94.88% ± 1.22% to 32.48% ± 0.71%. This resulted from the saturation of active functional groups available on the adsorbent at high adsorbate concentrations (Nadarajah et al., 2021). Moreover, high removal efficiencies observed at low dye concentrations could be described according to the ratio of MB molecules to the availability of adsorption sites (Labaran et al., 2019).

3.3.3. Influence of adsorbent dosage

The adsorbent dosage played an important role in the adsorption process. As shown in Fig. 7, as the PSC dosage was increased, q_e decreased, and the removal efficiency increased. Similar trends were reported by previous experiments using coconut coir dust (Etim et al., 2016) and the peel of *Citrus limetta* fruit (Shakoor and Nasar, 2016) as adsorbents for adsorptive removal of MB. As the adsorbent dosage was increased from 1 g/L to 5 g/L, the removal efficiency showed a rapid increment. However, a further increase in the adsorbent dosage only caused a slight increase in the removal efficiency, and the removal efficiency was stabilized at 98%. The increasing trend of the removal efficiency could be explained

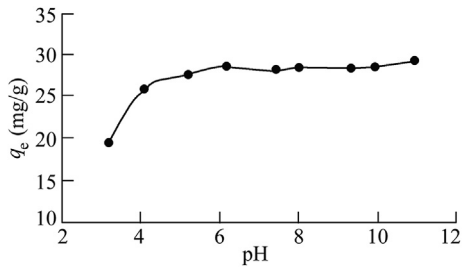

Fig. 5. Effect of initial pH on MB adsorption to PSC.

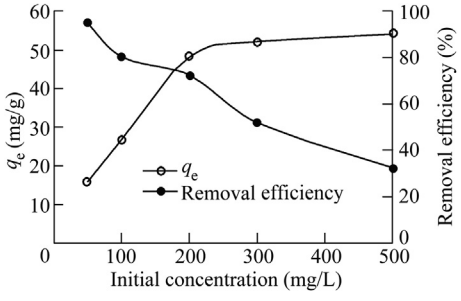

Fig. 6. Effect of initial MB concentration on adsorption with PSC.

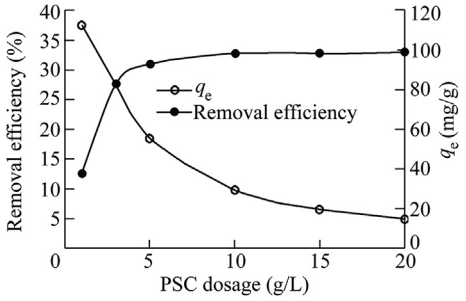

Fig. 7. Effect of PSC dosage on MB adsorption.

by the expansion of surface area with an increase in the adsorbent dosage, causing more available binding sites for the adsorption (Shakoor and Nasar, 2016). Due to the increment in the adsorbent dosage, q_e decreased gradually. This is understandable according to the definition of q_e (the adsorbate amount removed per unit weight of adsorbent) (Nadarajah et al., 2021). Moreover, as the adsorbent dosage is increased, there is a chance for the occurrence of the interactions (aggregation or agglomeration) among adsorbent particles, which could lead to the decreased total surface area (Shakoor and Nasar, 2016).

3.3.4. Influence of temperature

The adsorption behavior was studied within a temperature range from 30°C to 50°C. Fig. 8 shows the effect of temperature on the MB adsorption performance with PSC. Both q_e and the removal efficiency were observed to decrease as the temperature was increased from 30°C to 50°C. The maximum q_e and removal efficiency were found at 30°C, with values of (31.47 ± 0.01) mg/g and 94.40% ± 0.04%, respectively. The minimum q_e and removal efficiency appeared at 0°C, with values of (30.99 ± 0.11) mg/g and 92.97% ± 0.04%, respectively. The high adsorption ability observed at low temperatures was due to the endothermic nature of the adsorption mechanisms that could be explained by thermodynamic analyses (see Section 3.6). A similar trend was previously reported for biosorption of MB using other biosorbents, such as the skin of bamboo shoot (Zhu et al., 2019) and *Citrus sinensis* bagasse (Bhatti et al., 2012). When the temperature is increased, the thermal motion of molecules becomes more active (Zhu et al., 2019). Thus, there was a low chance for MB adsorption with PSC at high temperatures. Moreover, intermolecular hydrogen bonds between the dye and adsorbent might become weak at high temperatures (Theng et al., 2020). Therefore, the attractive forces between the surface of the biosorbent and dye molecules are weak at high temperatures. Therefore, MB adsorption using PSC should be carried out at low temperatures to achieve an efficient dye removal performance.

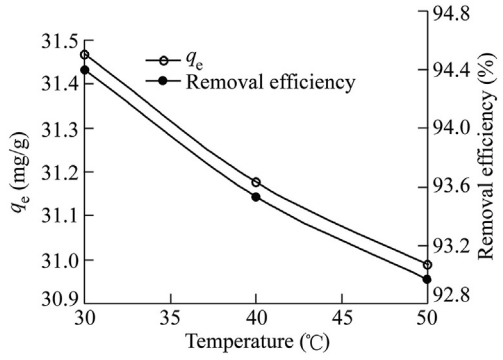

Fig. 8. Effect of temperature on MB adsorption.

3.4. Adsorption isotherm

Adsorption isotherm explains the distribution of dye molecules on the surface of the adsorbent at the equilibrium state of the adsorption. Three widely known isotherm models (Langmuir, Temkin, and Freundlich) were used to study the deposition nature of dye molecules on the surfaces of the biosorbents. Fig. A.2 in Appendix A shows the adsorption isotherms of PSC. The Langmuir model fitted the experimental data better (with a determination coefficient (R^2) of 0.998) than the Freundlich (R^2 = 0.930) and Temkin models (R^2 = 0.920). Thus, the adsorption mechanisms could be explained by the Langmuir model for an ideal homogeneous sorption scenario. Similar findings were obtained in previous studies on MB adsorption using the peel of *Citrus limetta* fruit (Shakoor and Nasar, 2016), *Casuarina equisetifolia* needle (Dahri et al., 2015), garlic straw (Kallel et al., 2016), and banana peel (Amela et al., 2012).

The Langmuir isotherm model explains that adsorption sites present on a specific adsorbent are equivalent and identical. Therefore, each adsorption site shows an equal affinity to the adsorbate. Moreover, a rigid layer with a thickness of only one molecule forms during the adsorption, and there is no more interaction or mitigation between the adsorbed molecules and ions after the adsorption. Therefore, no further sorption or desorption occurs once all adsorption sites are occupied (Ziyath, 2012). Accordingly, the adsorption of MB onto PSC was monolayer in nature. Due to the development of strong attractions between the adsorbent and adsorbate, this monolayer adsorption is important to better adsorptive performance (Nadarajah et al., 2021). The separation factor (R_L) is a parameter of the Langmuir model. This parameter indicates the characteristics of the adsorption process to be favorable ($0 < R_L < 1$), unfavorable ($R_L > 1$), linear ($R_L = 1$), or irreversible ($R_L = 0$) (Low and Tan, 2018). The R_L value obtained in this study for MB adsorption with PSC was 0.023, indicating the favorability of the adsorption process.

3.5. Adsorption kinetics

The Elovich, pseudo-first-order, and pseudo-second-order models were used to study the kinetic mechanisms. Fig. A.3 in Appendix A shows the adsorption kinetics fitted with these three kinetic models. Table 1 shows the obtained R^2 and parameter values of the three models. The pseudo-second-order

Table 1
Parameters and R^2 of pseudo-first-order, pseudo-second-order, and Elovich kinetic models.

C_e (mg/L)	Experimental q_e (mg/g)	Pseudo-first-order model			Pseudo-second-order model			Elovich model		
		Calculated q_e (mg/g)	k_1 (L/min)	R^2	Calculated q_e (mg/g)	k_2 (g/(mg·min))	R^2	α (g/(mg·min))	β (g/mg)	R^2
100	30.09	5.676	0.002	0.405	30.39	0.002	0.999	15.056	0.25	0.84
300	67.99	41.190	0.005	0.623	68.02	0.000	0.998	14.487	0.11	0.96
200	59.03	988.090	0.003	0.401	57.14	0.000	0.994	4 063.100	0.27	0.14

Note: C_e is the equilibrium concentration; k_1 and k_2 are the rate constants of the pseudo-first-order and pseudo-second-order models, respectively; α is the rate of initial adsorption; and β is the desorption constant.

Table 2
Thermodynamic parameters for MB adsorption by PSC.

Temperature (K)	ΔG_0 (kJ/mol)	ΔH_0 (kJ/mol)	ΔS_0 (J/mol)
303	−4.344	−9.950	−18.55
313	−4.159	−9.950	−18.55
323	−3.974	−9.950	−18.55

kinetic model fitted the adsorption data well with $R^2 \geq 0.994$ at all different MB concentrations. Moreover, compared to other two models, the q_e values calculated with the pseudo-second-order model were more similar to the q_e values that were directly calculated with the experimental data. This indicated that the pseudo-second-order kinetic model was more suitable to explain the MB adsorption onto PSC.

The pseudo-second-order kinetic model was also reported as a suitable kinetic model for MB adsorption using other biosorbents, such as durian skin (Anisuzzaman et al., 2015), sugarcane bagasse (Siqueira et al., 2020), the peel of citrus fruit (Dutta et al., 2011), and the needles of *C. equisetifolia* (Dahri et al., 2015). Thus, the adsorption mechanisms could be explained with the pseudo-second-order kinetic model. According to the pseudo-second-order model, the chemisorption process actively involves in the adsorption mechanisms (Dahri et al., 2015). It further explains that adsorption is determined by the concentration of ions on the surface of the adsorbent during adsorption (Amela et al., 2012). Moreover, chemisorption can be concluded as the rate controlling factor of the adsorption process. It also involves in the formation of valence forces by exchanging or sharing electrons between PSC and MB in the adsorptive removal process (Siqueira et al., 2020).

3.6. Adsorption thermodynamics

Adsorption thermodynamic studies are related to the energy change in the adsorbent due to the adsorption of MB. The experimental data collected at different temperatures (303 K, 313 K, and 323 K) were used to calculate the thermodynamic parameters: the Gibbs free energy of adsorption (ΔG_0), entropy change (ΔS_0), and enthalpy (ΔH_0) (Table 2). These parameters were calculated by plotting ln K_D versus $1/T$ (with K_D denoting the equilibrium constant and T representing the temperature) (Fig. 9), and all these parameters were negative in this study. Similar results were reported for the adsorptive removal of MB using pomegranate peel (Jawad et al., 2018) and *Cucumis sativus* peel (Shakoor and Nasar, 2017). At temperatures of 303 K, 313 K, and 323 K, the ΔG_0 values were −4.344 kJ/mol, −4.159 kJ/mol, and −3.974 kJ/mol, respectively. This explained the spontaneous nature of the adsorption process and confirmed the feasibility of the adsorption mechanisms (Siqueira et al., 2020). The negative ΔG_0 values also indicated that low temperatures were suitable for adsorption (Jawad et al., 2018). As the temperature was increased, the absolute value of ΔG_0 decreased. This revealed that the adsorption mechanisms were more spontaneous at lower temperatures (Dahri et al., 2015). The negative value of ΔH_0 (−9.950 kJ/mol) was due to the exothermic nature of the adsorption process (Nadarajah et al., 2021). The negative ΔS_0 value indicated that the randomness at the solid−solution interface decreased during adsorption (Jawad et al., 2018).

3.7. Understanding of adsorption-limiting factors

The rate-limiting effect influences MB movement onto the surface of the adsorbent and into its pore space. The intra-particle diffusion process is most probably responsible for the transport of adsorbate ions or molecules from the solution to the solid phase of the adsorbent, and it is often the rate-limiting factor (Kini et al., 2014). The involvement of intra-particle diffusion can be tested with the Weber−Morris model. The amount of MB adsorbed per unit mass of PSC at time t (q_t) was plotted against the square root of time ($t^{1/2}$) (Fig. 10(a)). At all three tested MB concentrations, two distinguished linear sections with different slopes were identified. This indicated that the adsorption process included two steps (Kini et al., 2014). This multi-linear phenomenon was

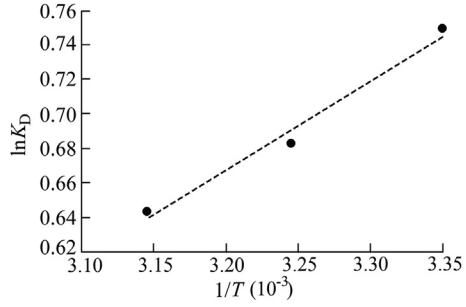

Fig. 9. Thermodynamic analysis of MB adsorption with PSC.

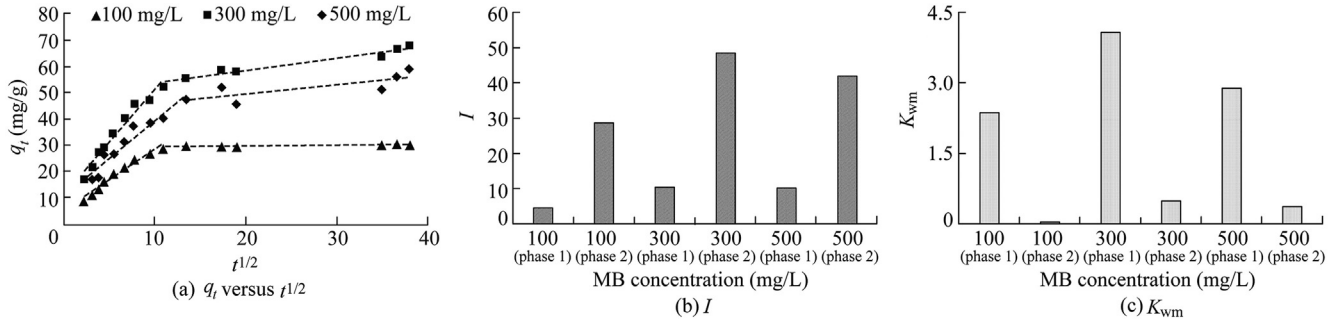

Fig. 10. Rate-limiting factor analysis of MB adsorption with PSC.

also observed during MB adsorption onto palm tree flower powder (Kini et al., 2014) and tea stem (Lee et al., 2019).

If the rate-limiting process is only dependent on intraparticle diffusion, the regression of q_t versus $t^{1/2}$ should be a linear curve, and the curve should go through the point of origin (Hameed and Ahmad, 2009). Although two linear phases were identified at each MB concentration, they did not go through the origin. This indicated that intraparticle diffusion was not the sole step that limited the adsorption rate (Hameed and Ahmad, 2009), and complex reaction mechanisms should be involved in MB removal with PSC (Singh et al., 2018). According to the Weber−Morris model, the initial part of the plot of q_t versus $t^{1/2}$ represents surface adsorption, and the latter part indicates intraparticle diffusion (Singh et al., 2018). The presence of the two distinct parts confirmed that intraparticle diffusion and surface adsorption jointly controlled MB adsorption with PSC. The high slopes of the first linear part were caused by the rapid movement of the adsorbate from the aqueous phase to the adsorbent surface due to the attractive forces that created by the surface functional properties of PSC. The low slopes of the second linear part resulted from the influence of the rate of intraparticle diffusion after a long duration of reaction (Nadarajah et al., 2021).

Fig. 10(b) and (c) show the intercepts (I) and slopes (K_{wm}) of the curves of Fig. 10(a) in different linear phases, respectively. At a particular MB concentration, the K_{wm} values of the second linear portion were always lower than those of the first linear portion. This indicated that the boundary layer impact was more significant in the second phase of the adsorption process than in the first phase (Nadarajah et al., 2021). The intercept value (I) can be used to understand the boundary layer thickness. At all tested MB concentrations, the obtained I values were greater in the second linear phase than in the first linear phase. This revealed that the rate-limiting factors were the intraparticle diffusion rate and boundary layer thickness (Nadarajah et al., 2021). Therefore, the rate-limiting effect of overall adsorption performance was dependent on intraparticle diffusion and boundary layer thickness on the adsorbent surface.

4. Conclusions

Biosorbents are cost effective adsorbents that can be successfully utilized for the adsorptive removal of industrial dyes from contaminated wastewater. Therefore, this study comprehensively investigated five biosorbents with limited scientific understanding for MB dye removal. The selected five biosorbents had different MB adsorption performances due to their different surface functional properties. Moreover, the XRD and pH_{pzc} analyses showed that the five biosorbents were different in crystallographic features and surface charge distribution. Of the selected biosorbents, PSC exhibited the highest adsorption performance (27.673 mg/g). Thus, PSC was selected for detailed analyses to understand the adsorption mechanisms. The FTIR and XRD analyses conducted before and after the adsorption of the dye indicated the impacts of functional groups, such as C−H bending, N−O stretching, and some carbonyl and hydroxyl, and some changes occurred in crystal structures. Therefore, to improve the MB removal performance of PSC, the identified important functional groups should be systematically enriched.

According to the adsorption isotherm studies, the Langmuir model well fitted the experimental data, indicating the monolayer adsorptive removal of MB with PSC. The pseudo-second-order kinetic model demonstrated that chemisorption was actively involved in the adsorptive removal process. The thermodynamic analysis revealed that the adsorption mechanisms were exothermic and spontaneous. The Weber−Morris model explained that the thickness of the boundary layer and the rate of intraparticle diffusion were significant rate-limiting factors. The biosorbent used in this study deepens our knowledge to expand the use of biosorbents for dye removal from water in the future. However, it is highly needed to increase the adsorption ability of biosorbents via suitable modifications to meet the industrial demand.

Declaration of competing interest

The authors declare no conflicts of interest.

Acknowledgements

The authors would like to appreciate the Department of Agricultural Engineering, Faculty of Agriculture, University of Jaffna, Sri Lanka, for providing resources and financial support. We would like to extend our gratitude to the Department of Civil Engineering, Faculty of Engineering, University of Jaffna, for providing instrumental support. The

contributions given by Dr. G. Sashikesh for FTIR analysis and Dr. M. Thanihaichelvan for XRD analysis are highly acknowledged.

Appendix A. Supplementary data

Supplementary data to this article can be found online at https://doi.org/10.1016/j.wse.2022.12.006.

References

Ahmad, N., Azli, A.F.A., Mat, N.C., Nawi, F.N.F.M., Othman, M.H., 2016. Adsorption of methylene blue in aqueous solution by *Musa paradisiaca* stem powder. ARPN J. Eng. Appl. Sci. 11, 6186−6190.

Amela, K., Hassen, M.A., Kerroum, D., 2012. Isotherm and kinetics study of biosorption of cationic dye onto banana peel. Energy Proc. 19, 286−295. https://doi.org/10.1016/j.egypro.2012.05.208.

Anisuzzaman, S.M., Joseph, C.G., Krishnaiah, D., Bono, A., Ooi, L.C., 2015. Parametric and adsorption kinetic studies of methylene blue removal from simulated textile water using durian (*Durio zibethinus murray*) skin. Water Sci. Technol. 72(6), 896−907. https://doi.org/10.2166/wst.2015.247.

Benkhaya, S., Harfi, S.E., Harfi, A.E., 2018. Classifications, properties and applications of textile dyes: A review. Applied Journal of Environmental Engineering Science 3(3), 311−320. https://doi.org/10.48422/IMIST.PRSM/ajees-v3i3.9681.

Bhatti, H.N., Akhtar, N., Saleem, N., 2012. Adsorptive removal of methylene blue by low-cost *Citrus sinensis* bagasse: Equilibrium, kinetic and thermodynamic characterization. Arabian J. Sci. Eng. 37(1), 9−18. https://doi.org/10.1007/s13369-011-0158-1.

Dahri, M.K., Kooh, M.R.R., Lim, L.B., 2015. Application of *Casuarina equisetifolia* needle for the removal of methylene blue and malachite green dyes from aqueous solution. Alex. Eng. J. 54(4), 1253−1263. https://doi.org/10.1016/j.aej.2015.07.005.

Dutta, S., Bhattacharyya, A., Ganguly, A., Gupta, S., Basu, S., 2011. Application of response surface methodology for preparation of low-cost adsorbent from citrus fruit peel and for removal of methylene blue. Desalination 275(1−3), 26−36. https://doi.org/10.1016/j.desal.2011.02.057.

Etim, U.J., Umoren, S.A., Eduok, U.M., 2016. Coconut coir dust as a low cost adsorbent for the removal of cationic dye from aqueous solution. J. Saudi Chem. Soc. 20, S67−S76. https://doi.org/10.1016/j.jscs.2012.09.014.

Ghosh, I., Kar, S., Chatterjee, T., Bar, N., Das, S.K., 2021a. Adsorptive removal of Safranin-O dye from aqueous medium using coconut coir and its acid-treated forms: Adsorption study, scale-up design, MPR and GA-ANN modeling. Sustainable Chemistry and Pharmacy 19, 100374. https://doi.org/10.1016/j.scp.2021.100374.

Ghosh, I., Kar, S., Chatterjee, T., Bar, N., Das, S.K., 2021b. Removal of methylene blue from aqueous solution using *Lathyrus sativus* husk: Adsorption study, MPR and ANN modelling. Process Saf. Environ. Protect. 149, 345−361. https://doi.org/10.1016/j.psep.2020.11.003.

Ghosh, K., Bar, N., Biswas, A.B., Das, S.K., 2019. Removal of methylene blue (aq) using untreated and acid-treated eucalyptus leaves and GA-ANN modelling. Can. J. Chem. Eng. 97(11), 2883−2898. https://doi.org/10.1002/cjce.23503.

Ghosh, K., Bar, N., Biswas, A.B., Das, S.K., 2021c. Elimination of crystal violet from synthetic medium by adsorption using unmodified and acid-modified eucalyptus leaves with MPR and GA application. Sustainable Chemistry and Pharmacy 19, 100370. https://doi.org/10.1016/j.scp.2020.100370.

Ghosh, K., Bar, N., Roymahapatra, G., Biswas, A.B., Das, S.K., 2022. Adsorptive removal of toxic malachite green from its aqueous solution by *Bambusa vulgaris* leaves and its acid-treated form: DFT, MPR and GA modeling. J. Mol. Liq. 363, 119841. https://doi.org/10.1016/j.molliq.2022.119841.

Hameed, B.H., Ahmad, A.A., 2009. Batch adsorption of methylene blue from aqueous solution by garlic peel, an agricultural waste biomass. J. Hazard Mater. 164(2−3), 870−875. https://doi.org/10.1016/j.jhazmat.2008.08.084.

Jawad, A.H., Waheeb, A.S., Rashid, R.A., Nawawi, W.I., Yousif, E., 2018. Equilibrium isotherms, kinetics, and thermodynamics studies of methylene blue adsorption on pomegranate (*Punica granatum*) peels as a natural low-cost biosorbent. Desalination Water Treat. 105, 322−331. https://doi.org/10.5004/dwt.2018.22021.

Kallel, F., Chaari, F., Bouaziz, F., Bettaieb, F., Ghorbel, R., Chaabouni, S.E., 2016. Sorption and desorption characteristics for the removal of a toxic dye, methylene blue from aqueous solution by a low cost agricultural by-product. J. Mol. Liq. 219, 279−288. https://doi.org/10.1016/j.molliq.2016.03.024.

Khan, M., Motiar, R., Sahoo, B., Mukherjee, A.K., Naskar, A., 2019. Biosorption of acid yellow-99 using mango (*Mangifera indica*) leaf powder, an economic agricultural waste. SN Appl. Sci. 1(11), 1−15. https://doi.org/10.1007/s42452-019-1537-6.

Kini, M.S., Saidutta, M.B., Murty, V.R., 2014. Studies on biosorption of methylene blue from aqueous solutions by powdered palm tree flower (*Borassus flabellifer*). Int. J. Chem. Eng. 306519. https://doi.org/10.1155/2014/306519, 2014.

Labaran, A.N., Zango, Z.U., Armaya'u, U., Garba, Z.N., 2019. Rice husk as biosorbent for the adsorption of methylene blue. Sci. World J. 14(2), 66−70.

Lakshmipathy, R., Sarada, N.C., 2015. Methylene blue adsorption onto native watermelon rind: Batch and fixed bed column studies. Desalination Water Treat. 57, 10632−10645. https://doi.org/10.1080/19443994.2015.1040462.

Lee, T.C., Wang, S., Huang, Z., Mo, Z., Wang, G., Wu, Z., et al., 2019. Tea stem as a sorbent for removal of methylene blue from aqueous phase. Adv. Mater. Sci. Eng. 9723763. https://doi.org/10.1155/2019/9723763, 2019.

Low, S.K., Tan, M.C., 2018. Dye adsorption characteristic of ultrasound pretreated pomelo peel. J. Environ. Chem. Eng. 6(2), 3502−3509. https://doi.org/10.1016/j.jece.2018.05.013.

Nadarajah, K., Bandala, E.R., Zhang, Z., Mundree, S., Goonetilleke, A., 2021. Removal of heavy metals from water using engineered hydrochar: Kinetics and mechanistic approach. J. Water Proc. Eng. 40, 101929. https://doi.org/10.1016/j.jwpe.2021.101929.

Park, D., Yun, Y.S., Park, J.M., 2010. The past, present, and future trends of biosorption. Biotechnol. Bioproc. E 15, 86−102. https://doi.org/10.1007/s12257-009-0199-4.

Pavan, F.A., Gushikem, Y., Mazzocato, A.C., Dias, S.L., Lima, E.C., 2007. Statistical design of experiments as a tool for optimizing the batch conditions to methylene blue biosorption on yellow passion fruit and Mandarin peels. Dyes and Pigments 72(2), 256−266. https://doi.org/10.1016/j.dyepig.2005.09.001.

Rani, K.C., Naik, A., Chaurasiya, R.S., Raghavarao, K.S.M.S., 2017. Removal of toxic Congo red dye from water employing low-cost coconut residual fiber. Water Sci. Technol. 75(9), 2225−2236. https://doi.org/10.2166/wst.2017.109.

Rehman, R., Farooq, S., Mahmud, T., 2019. Use of agro-waste *Musa acuminata* and *Solanum tuberosum* peels for economical sorptive removal of Emerald green dye in ecofriendly way. J. Clean. Prod. 206, 819−826. https://doi.org/10.1016/j.jclepro.2018.09.226.

Shakoor, S., Nasar, A., 2016. Removal of methylene blue dye from artificially contaminated water using citrus limetta peel waste as a very low cost adsorbent. J. Taiwan Inst. Chem. Eng. 66, 154−163. https://doi.org/10.1016/j.jtice.2016.06.009.

Shakoor, S., Nasar, A., 2017. Adsorptive treatment of hazardous methylene blue dye from artificially contaminated water using *Cucumis sativus* peel waste as a low-cost adsorbent. Groundwater for Sustainable Development 5, 152−159. https://doi.org/10.1016/j.gsd.2017.06.005.

Stjepanović, M., Velić, N., Galić, A., Kosović, I., Jakovljević, T., Habuda-Stanić, M., 2021. From waste to biosorbent: Removal of Congo red from water by waste wood biomass. Water 13(3), 279. https://doi.org/10.3390/w13030279.

Singh, R., Lata, S., Balasubramanian, P., 2018. Biosorption characteristics of methylene blue and malachite green from simulated wastewater onto *Carica papaya* wood biosorbent. Surface. Interfac. 10, 197−215.

Siqueira, T.C., Zanette da Silva, I., Rubio, A.J., Bergamasco, R., Gasparotto, F., Aparecida de Souza Paccola, E., et al., 2020. Sugarcane bagasse as an efficient biosorbent for methylene blue removal: Kinetics,

isotherms and thermodynamics. Int. J. Environ. Res. Publ. Health 17(2), 526. https://doi.org/10.3390/ijerph17020526.

Theng, M.L., Tan, L.S., Siaw, W.C., 2020. Adsorption of methylene blue and Congo red dye from water onto cassava leaf powder. Progress in Energy and Environment 12, 11−21.

Vijayakumar, G., Dharmendrirakumar, M., Renganathan, S., Sivanesan, S., Baskar, G., Elango, K.P., 2009. Removal of Congo red from aqueous solutions by Perlite. Clean Soil Air Water 37(4−5), 355−364. https://doi.org/10.1002/clen.200800228.

Zhao, C., Wang, B., Theng, B.K., Wu, P., Liu, F., Wang, S., Zhang, X., 2021. Formation and mechanisms of nano-metal oxide-biochar composites for pollutants removal: A review. Sci. Total Environ. 767, 145305. https://doi.org/10.1016/j.scitotenv.2021.145305.

Zhu, L., Zhu, P., You, L., Li, S., 2019. Bamboo shoot skin: Turning waste to a valuable adsorbent for the removal of cationic dye from aqueous solution. Clean Technol. Environ. Policy 21(1), 81−92. https://doi.org/10.1007/s10098-018-1617-0.

Ziyath, M., 2012. Removal of Toxic Metals in a Multi Metal System Using Sorbents for Potential Application to Urban Stormwater Treatment. Queensland University of Technology, Brisbane. Ph.D. Dissertation.